Syngas Production by Catalytic Pyrolysis of Rice Straw over Modified Ni-based Catalyst

Kui Lan, Zhenhua Qin, Zeshan Li, Rui Hu, Xianzhou Xu, Weitao He, and Jianfen Li *

Ni-xLa/Al_2O_3-MgO-sawdust char catalysts were prepared by modifying the Ni/Al_2O_3 catalyst from two aspects of support and active components. The effect of Al_2O_3, MgO, sawdust char molar ratio, and La content of catalysts on syngas (H_2 + CO) production in the catalytic pyrolysis of rice straw was investigated in a horizontal fixed-bed quartz tube reactor. Furthermore, the stability of catalysts with the optimum catalytic performance was tested and compared with that of the Ni/Al_2O_3 catalysts. X-ray diffraction, X-ray fluorescence, field emission scanning electron microscopy, energy disperse X-ray, and Brunauer-Emmett-Teller analyses were applied to understand the physiochemical properties of the supports and catalysts. The study revealed that the supports were composed of many irregular flaky particles and thus formed many pores. Moreover, the addition of La decreased the particle size of $NiAl_2O_4$ and increased the active metal surface of the Ni/Al_2O_3-MgO-sawdust catalysts. When the molar ratio of Al_2O_3, MgO, and sawdust char was 1:1:1 and the La content was 10 wt% (dry weight basis), the catalysts presented the highest syngas concentration of 78.9 vol% and the most stable performance during the catalytic pyrolysis process.

Keywords: Modified catalyst; Catalytic pyrolysis; Rice straw; Syngas

*Contact information: School of Chemical and Environmental Engineering, Wuhan Polytechnic University, Wuhan 430023, China; *Corresponding author: lijfen@163.com*

INTRODUCTION

Biomass is a carbon neutral green energy that has great potential in reducing fossil fuel consumption and greenhouse gas emissions (Huang *et al*. 2016) because of its renewability, abundance, and low N/S pollution characteristics (Shen *et al*. 2013). Hence, the rational exploitation and utilization of biomass resources can effectively alleviate the pressure of fossil energy shortage and the problem of global warming (Chen *et al*. 2019). One of the aspects of biomass utilization is the production of syngas (H_2+CO), which is an important gas mixture that can be used as a fuel in an internal combustion engine for power generation, as well as in a boiler for heat generation or a feedstock for Fischer-Tropsch synthesis (Demirbas 2009; Hu *et al*. 2016). Among various biomass resources utilization technologies, pyrolysis is considered one of the most potential thermochemical technologies in terms of the efficient and clean conversion of biomass into syngas (Dong *et al*. 2019). However, the presence of tar by-products in syngas hinders the large-scale commercial application of biomass pyrolysis technology (Wang *et al*. 2017; Yang *et al*. 2017). Biomass tar contains many harmful chemicals that can condense on the pipe wall and clog filters or downstream devices, leading to equipment failure (Beneroso *et al*. 2016). In addition, it wastes energy and can even endanger people's health. Therefore, it is crucial to effectively remove the tar from the syngas of biomass pyrolysis.

At present, several technologies for removing the tar from the syngas have been examined, such as physical treatment (Paethanom *et al*. 2012), thermal pyrolysis (Fagbemi *et al*. 2001), plasma-assisted pyrolysis (Zhu *et al*. 2016), and catalytic pyrolysis (Artetxe *et al*. 2017). Among these methods, catalytic pyrolysis, which can degrade tar at 600 to 900 °C, is regarded as a cost-effective method because of its high reliability and fast reaction rate (Zhang *et al*. 2004; Li *et al*. 2014; Shen *et al*. 2018). Currently, a variety of catalysts such as olivine (Michel *et al.* 2013), dolomite (Yu et al. 2009), zeolites (Shao *et al.* 2018), noble metals (Furusawa and Tsutsumi 2005), non-nickel transition metals (Li et al. 2013), and nickel-based catalysts (He *et al.* 2009), have been heavily investigated in biomass catalytic pyrolysis. Noble metal catalysts have the dual characteristics of superior catalytic performance and high cost. Ni-based catalysts are widely used in tar removal from the syngas of biomass pyrolysis (Dong *et al*. 2016; Hu *et al*. 2016) due to their good catalytic activity/cost ratio (Zhang *et al*. 2018). However, it is worth noting that the combination of high temperature and pressure, hydrocarbons, and impurities creates a harsh environment for nickel-based catalysts. This makes the usage of nickel-based catalysts challenging due to deactivation from coke deposition and sintering (Melo and Morlanés 2005; Sehested 2006; Li *et al*. 2009). Hence, it is vital to develop high activity catalysts with strong capacity to resist carbon deposition and sintering.

Various metal additives, such as transition metals and alkaline earth metals, can be added to the Ni-based catalysts. According to Świerczyński *et al.* (2007), during the steam reforming of toluene, the presence of Ni-Fe alloy and (Ni, Mg) O solid solution restrained the formation of carbon deposition on Ni/olivine catalysts. Wang *et al.* (2013) studied the performance of Ni-Co/Al_2O_3 catalysts in pyrolysis of cedar wood. The results demonstrated that the Ni-Co/Al_2O_3 catalysts with the Ni/Co optimum mole ratio of 0.25 revealed much higher catalytic performance in terms of catalytic activity, the resistance of carbon deposition and catalysts life compared to the Ni/Al_2O_3 and Co/Al_2O_3 catalysts. Li *et al.* (2013) investigated the effect of MgO addition on the performance of Ni/γ-Al_2O_3 catalysts for catalytic pyrolysis of rice straw to produce hydrogen-rich syngas. They found that MgO improved the catalytic activity of Ni/γ-Al_2O_3 catalysts and behaved as a promoter for the water gas shift (WGS) reaction.

Another important parameter promoting the activity and stability of catalysts is the selection of suitable supports (Li *et al*. 2015) because they can facilitate the dispersion of active metal and restrain the aggregation of metal particles efficiently in addition to participate in the catalytic reaction (Wang *et al*. 2016; Sharma *et al*. 2017; Zhang *et al*. 2017). In general, metallic oxide (Al_2O_3, MgO, CaO, and ZrO_2), natural minerals (dolomite, olivine), and zeolites (SBA-15, ZSM-5, and ZY) are frequently applied as the support of Ni-based catalysts. Among these supports, the most widely used is alumina (Zhang *et al*. 2018), which has a high specific surface area to provide a suitable Ni dispersion, and its mechanical strength ensures the stability of the catalysts (Charisiou *et al*. 2017). Unfortunately, the abundant amounts of acid sites on the surface of alumina promote coke formation and rapid deactivation of the Ni/Al_2O_3 catalysts (Chen *et al*. 2019). Therefore, research on the modification of Al_2O_3 support has aroused an increasing interest. In the study of Ashok and Kawi (2014), a new Fe_2O_3-Al_2O_3 support material was synthesized and used to prepare the Ni/Fe_2O_3-Al_2O_3 catalysts. In the toluene reforming test, the Ni/Fe_2O_3-Al_2O_3 catalysts with 500 °C calcination temperature exhibited more than 90% toluene conversion in 26 h with a H_2/CO ratio of 4.5, which performed a superior catalytic activity and stability than Ni/Fe_2O_3 and Ni/Al_2O_3 catalysts. Shi *et al.* (2019) modified alumina with activated carbon (AC) and studied the effect of the Ni-Fe/AC-Al_2O_3 catalysts

on pyrolysis of rape straw to produce syngas. They reported that after using the Ni-Fe/AC-Al_2O_3 catalysts, the syngas yield increased to 2.22 Nm^3/kg, which was more than the Ni-Fe/AC (1.93 Nm^3/kg) and Ni-Fe/Al_2O_3 (1.69 Nm^3/kg) catalysts. Moreover, the Ni-Fe/AC-Al_2O_3 catalysts exhibited stronger resistance to deactivation than the single-supported catalysts. Recently, the use of by-product char of biomass pyrolysis/gasification as the catalysts support has attracted considerable attention due to its relatively low cost and superior physicochemical property (Guo *et al*. 2018). However, the higher mass loss of the catalysts was found during the catalytic reforming process (Dong *et al*. 2019). Alkaline earth metal oxides, such as MgO, were also commonly used as support because they can neutralize the acid sites of alumina (Sánchez-Sánchez *et al*. 2007), thereby inhibiting the formation of carbon deposition. To the authors' knowledge, when some metal oxides and biomass char are used as support alone, they can facilitate the catalysts to exhibit excellent catalytic performance. However, there also exist some defects. It may be a new research direction that combines alkaline earth metal oxides, biomass char, and Al_2O_3 as composite supports to improve the catalytic performance of Ni/Al_2O_3 catalysts; currently there are few well-established studies about this aspect.

Therefore, in the present work, a novel nickel-based catalyst was developed by modifying the conventional Ni/Al_2O_3 catalysts from the two directions of metal additives and support. The developed catalysts were applied to syngas production from catalytic pyrolysis of rice straw. The Al_2O_3-MgO-sawdust char (AMS) supports were prepared by co-precipitation method, then the optimum molar ratio of Al_2O_3, sawdust char, and MgO was investigated. The metal La was doped into the catalysts to change the interaction of metal-support and the structure of catalysts. In addition, the dependence of La content (0, 2, 4, 6, 8, and 10 wt% (dry weight basis)) together with the performance of the catalysts was investigated.

EXPERIMENTAL

Materials

The rice straw (RS), collected from Wuhan, China, was chosen as the feedstock of catalytic pyrolysis in this study. The rice straw was crushed and sieved to obtain a particle size of 0.3 to 0.45 mm prior to being oven-dried for 12 h at 105 ℃. The results of ultimate and proximate analyses of the materials (Table 1) were measured by an elemental analyzer (Flash 2000; Thermo Fisher Scientific, Waltham, MA, USA) and the procedures of GB/T 28731 (2012), respectively. The aluminium nitrate, magnesium nitrate, nickel nitrate, and aqueous ammonia were purchased from Sinopharm Chemical Reagent Co., Ltd. (Shanghai, China). The lanthanum nitrate and carbamide were purchased from Aladdin Industrial Corporation (Shanghai, China). The sawdust char were obtained by pyrolysis of sawdust under a nitrogen gas flow rate of 500 mL/min from room temperature to 700 ℃ at a heating rate of 10 ℃/min in a tube furnace and maintained for 2 h to ensure the complete pyrolysis.

Table 1. Proximate and Ultimate Analyses of the Rice Straw

Materials	Ultimate Analysis (wt%)					Proximate Analysis (wt%)			
	C	H	O*	N	S	M	A	V	FC
Rice straw	40.85	5.58	53.47	0.08	< 0.01	9.3	8.4	77.82	4.48
* by difference; M: Moisture; V: Volatile matter; A: Ash; FC: Fixed Carbon									

Catalysts Preparation

Preparation of supports

The AMS supports were prepared by the co-precipitation method. The appropriate amounts of aluminium nitrate, magnesium nitrate, and sawdust char (SC) were firstly dissolved in 200 mL deionized water with vigorous stirring for 30 min. After the mixture was evenly dispersed, the pH value of the solution was slowly adjusted to 10 with aqueous ammonia (25%) and the solution was further stirred for 3 h to complete the precipitation process. Then, the mixture solution was dried at 110 ℃ in an oven for 48 h after standing at ambient temperature for 6 h. Finally, the AMS supports were obtained after the support precursors were calcined under a nitrogen gas atmosphere from room temperature to 800 ℃ at a heating rate of 10 ℃/min in a tube furnace and kept stable for 3 h. A series of molar ratios of Al_2O_3 to MgO and SC were designed as 5:1:1, 4:1:1, 3:1:1, 2:1:1, and 1:1:1. The as-prepared catalyst supports were denoted as AMS-1, AMS-2, AMS-3, AMS-4, and AMS-5, respectively.

Loading of active metal

A series of Ni-based catalysts with the Ni loading of 10 wt% and various La content were prepared by co-precipitation method. A total of 5 g AMS supports were mixed with the solution containing the required amount of nickel nitrate, lanthanum nitrate, and carbamide in a 250-mL round-bottom flask. After that, the mixture solution was stirred for 2 h in an oil bath at 115 ℃ and then aged overnight. Subsequently, the mixture was dried at 110 ℃ for approximately 6 h in an oven after filtration washing to neutral with deionized water. The resulting powder was calcined under a nitrogen gas atmosphere from room temperature to 750 ℃ at a ramping rate of 10 ℃/min in a tube furnace and held for 2 h to yield NiO-*x*La/AMS catalysts, where *x* represents the different La contents (0, 2, 4, 6, 8, and 10 wt%).

Apparatus and Procedure

The whole lab-scale catalytic pyrolysis experimental device (Fig. 1) includes a gas supply system, pyrolysis reactor, gas purification system, syngas collection, and analysis system. The conversion of rice straw to syngas was completed in a horizontal fixed-bed quartz tube furnace reactor (3 kW, 240 V). The furnace can be slid left and right to control the finishing of pyrolysis reaction of rice straw. The reactor was approximately 60 mm in inner diameter, 1400 mm in total length, and 600 mm in the heating zone. Two quartz boats were applied to hold the rice straw and catalysts. Prior to the test, two quartz boats containing 2 g of rice straw and 1 g of catalysts were placed at one end of the quartz tube, and then the flanges at both ends of the furnace were closed. After that, nitrogen was used as the carrier gas and introduced continuously into the reactor with a flow rate of 200 mL/min for 20 min to provide an oxygen-free atmosphere. Then, the reactor was heated from ambient temperature to 700 ℃ at a ramping rate of 10 ℃/min and held for 20 min. Once the temperature of heating zone was preheated to 700 ℃, the two quartz boats with feedstock and catalysts were quickly pushed in. At the end of the reaction, the valves at both sides of the tube and nitrogen source were opened and the syngas was then carried into the gas sample bag by nitrogen gas. The gas analyzer (Gasboard-3100; Cubic-Ruiyi, Wuhan, China) was used to determine the gas composition and content. Each test was repeated several times to ensure the reliability of experimental data.

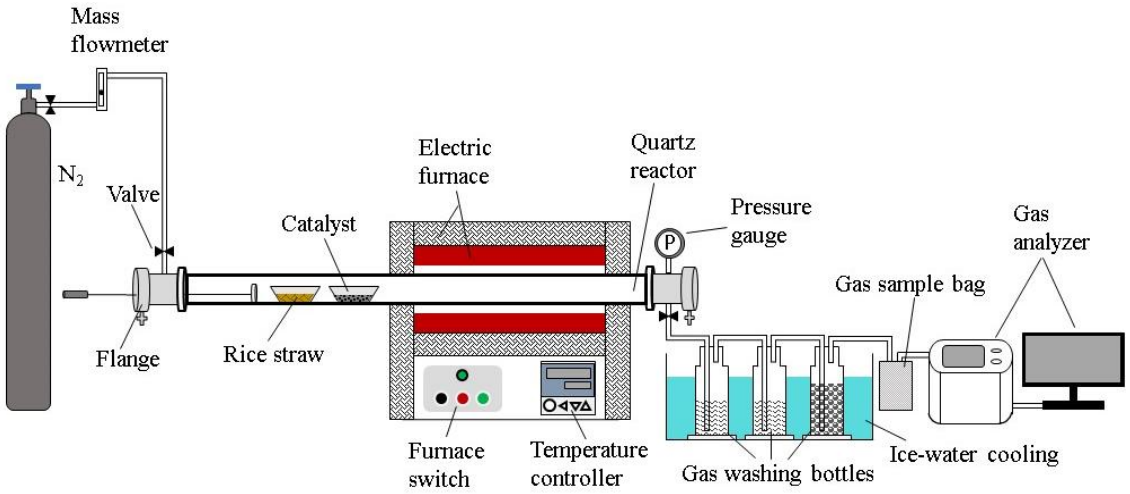

Fig. 1. Schematic diagram of the experimental system

Methods

The total metal loading levels (wt%) of the catalysts were quantified by X-ray fluorescence (EDX-720; Shimadzu, Kyoto, Japan) spectrometry. The crystalline phases were detected by X-ray diffraction (XRD-7000; Shimadzu, Kyoto, Japan). The textural properties of the catalysts, such as specific surface area, total pore volume, and average pore diameter, were investigated using the N_2 isothermal adsorption-desorption at 77 K by an automatic specific surface area and pore analyzer (ASAP 2460; Micromeritics, Atlanta, GA, USA). The morphological characteristics of catalysts were elucidated from the images, which were obtained using the field emission scanning electron microscope (JSM-7100F; JEOL, Ltd., Akishima, Japan) with energy dispersive X-ray (INCA X-MAX 250; OXFORD Instruments, Oxford, London). The gas product was collected with a gas sample bag and analyzed using an infrared gas analyzer (Gasboard-3100; Cubic-Ruiyi, Wuhan, China).

RESULTS AND DISCUSSION

Characterization of NiO/FA Catalyst

X-ray fluorescence (XRF) analysis

The elemental compositions of the support and catalysts are shown in Table 2. It should be pointed out that XRF cannot detect the carbon element; thus it was only used for qualitative analysis in this study. The XRF spectrum of the relative mass fraction ratio of Al_2O_3 and MgO was 2.28:1, which was close to the theoretical ratio of 2.53:1 (converted by the molar ratio of Al_2O_3 to MgO of 1:1), indicating that Al and Mg were successfully combined by the co-precipitation method. Meanwhile, the NiO content of the Ni/AMS-5 catalysts was 15.52 wt%, which was higher than the theoretical NiO loading of 12 wt% (converted by the theoretical Ni loading of 10 wt%). The NiO and La_2O_3 content of the Ni-10La/AMS-5 catalysts was also higher than the theoretical value. It has been commonly accepted that XRF is mainly for the micro-areas of material and is considered as a semi-quantitative analysis (Bo *et al*. 2008). Thus, there were some errors in the results. However, it can be seen that the relative contents of NiO and La_2O_3 were approximately equal, which

was consistent with the theoretical situation. Simultaneously, it revealed that Ni and La were successfully loaded onto the support.

Table 2. XRF Analyses of the Support and Catalysts

Sample	Elemental Compositions (wt%)				
	Al_2O_3	MgO	NiO	La_2O_3	Others
AMS-5	66.61	29.12	–	–	4.27
Ni/AMS-5	59.48	20.72	15.52	–	4.28
Ni-10La/AMS-5	44.07	19.42	16.76	15.71	4.04

X-ray diffraction (XRD) analysis

Figure 2 illustrates the XRD spectrograms of different supports and catalysts. It can be observed from (a) through (c) that there were several characteristic peaks around 2θ = 37.1°, 45.0°, 59.6°, and 65.8°, corresponding to the crystal structure of $MgAl_2O_3$. The appearance of the peaks at 2θ values of 37.0°, 44.9°, 59.7°, and 65.5° in (d) through (f) referred to $NiAl_2O_4$, which were indistinguishable in the XRD spectra with $MgAl_2O_4$ (Tichit *et al*. 1997).

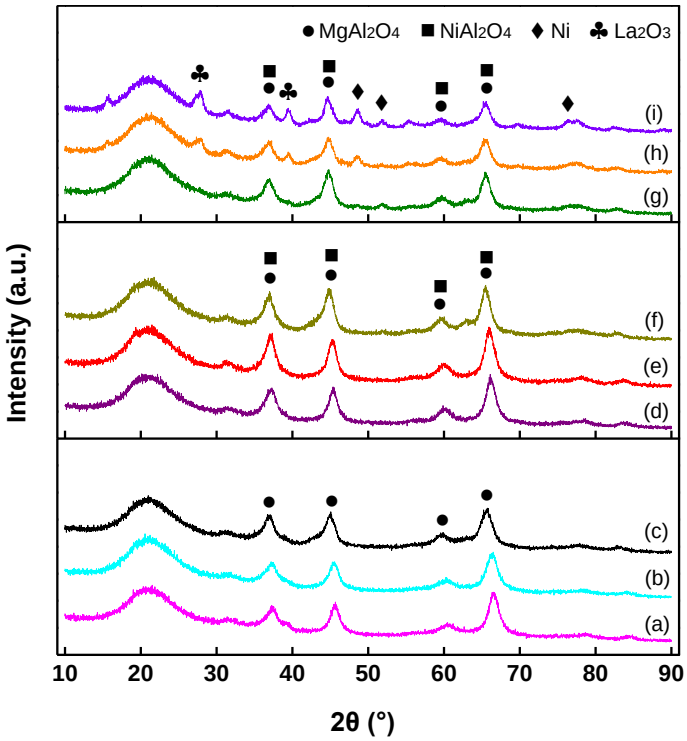

Fig. 2. XRD patterns of (a) AMS-1, (b) AMS-3, (c) AMS-5, (d) Ni/AMS-1, (e) Ni/AMS-3, (f) Ni/AMS-5, (g) Ni-2La/AMS-5, (h) Ni-6La/AMS-5, and (i) Ni-10La/AMS-5

For lanthanum promoted catalysts, some new diffraction lines were detected standing for the Ni and La_2O_3 phase. Moreover, the XRD spectra of (g) through (i) showed that the intensity of Ni phase diffraction peaks were gradually enhanced with the increase of La additive content. This indicated that the addition of La promoter was conducive to the formation of the Ni phase. R1 to R3 were the possible reactions that occurred during

the preparation of catalysts. The CO_2 produced by the decomposition of $Ni_2(OH)_2CO_3$ during calcination R3 would participate in reaction of R4. Subsequently, reaction of R5 occurred due to the presence of char in the support, and CO was produced that could reduce compound Ni to elemental Ni. Meanwhile, the higher the La content, the broader and weaker were the characteristic peaks of $NiAl_2O_4$ that appeared, demonstrating that the crystal particles became smaller (Surendar *et al*. 2017). This result revealed that La could effectively decrease the particle size of $NiAl_2O_4$.

It has been commonly believed that smaller metal particles engender more active sites, which are more conducive to catalytic pyrolysis reaction (Chen *et al*. 2019). It was noteworthy that no diffraction peaks of C appeared in the (a) through (i) XRD spectra. However, there was a weaker and wider peak around 30° in each spectrum, which was close to the main characteristic diffraction peak of C. This result indicated that the amorphous C formed during precipitation and calcination processes, leading to XRD cannot detect the diffraction peaks of C.

$$CO(NH_2)_2 + 3H_2O \rightarrow CO_2 + 2NH_3{\bullet}H_2O \quad (R1)$$

$$2Ni^{2+} + 4OH^- + CO_2 \rightarrow Ni_2(OH)_2CO_3 + H_2O \quad (R2)$$

$$Ni_2(OH)_2CO_3 \rightarrow NiO + CO_2 + H_2O \quad (R3)$$

$$La_2O_3 + CO_2 \rightarrow La_2O_2CO_3 \quad (R4)$$

$$La_2O_2CO_3 + C \rightarrow La_2O_3 + CO \quad (R5)$$

Field emission scanning electron microscopy (FESEM) and energy dispersive X-ray (EDX) analysis

The surface morphology of the support and catalysts were investigated by FESEM images, and the distribution of inorganic matters in the support and catalysts were analyzed by EDX, which are presented in Fig. 3 and Table 3. Figure 3(a) shows that the supports were composed by many irregular flaky particles and thus formed many pores. After loading Ni, the surface of catalysts became a relatively regular circular or elliptical flaky interlace structure, and some particles were filled in them as illustrated in Fig. 3(c). It can be seen from Fig. 2(d) through (f) that Ni was present in the form of $NiAl_2O_4$ in the Ni/AMS-5 catalysts. Therefore, the regular flaky structure was mainly generated by the interaction between active component and support. In contrast to Fig. 3(c), there were fewer particles between the flakes on the surface of the Ni-10La/AMS-5 catalysts in Fig. 3(e), which increased the amount of pores and facilitated more exposure of active sites to volatiles. The elemental composition analysis of the support and catalysts are listed in Table 3, revealing that the relative contents of Ni and La were close to the theoretical load of 10 wt%, indicating the active metal was successfully loaded on the support.

Table 3. Element Compositions of Support and Catalysts

Element (wt%)	AMS-5	Ni/AMS-5	Ni-10La/AMS-5
C	35.72	26.64	25.44
O	50.55	40.86	32.4
Mg	5.31	8.51	6.97
Al	8.42	15.43	17.89
Ni	–	8.56	8.93
La	–	–	8.37

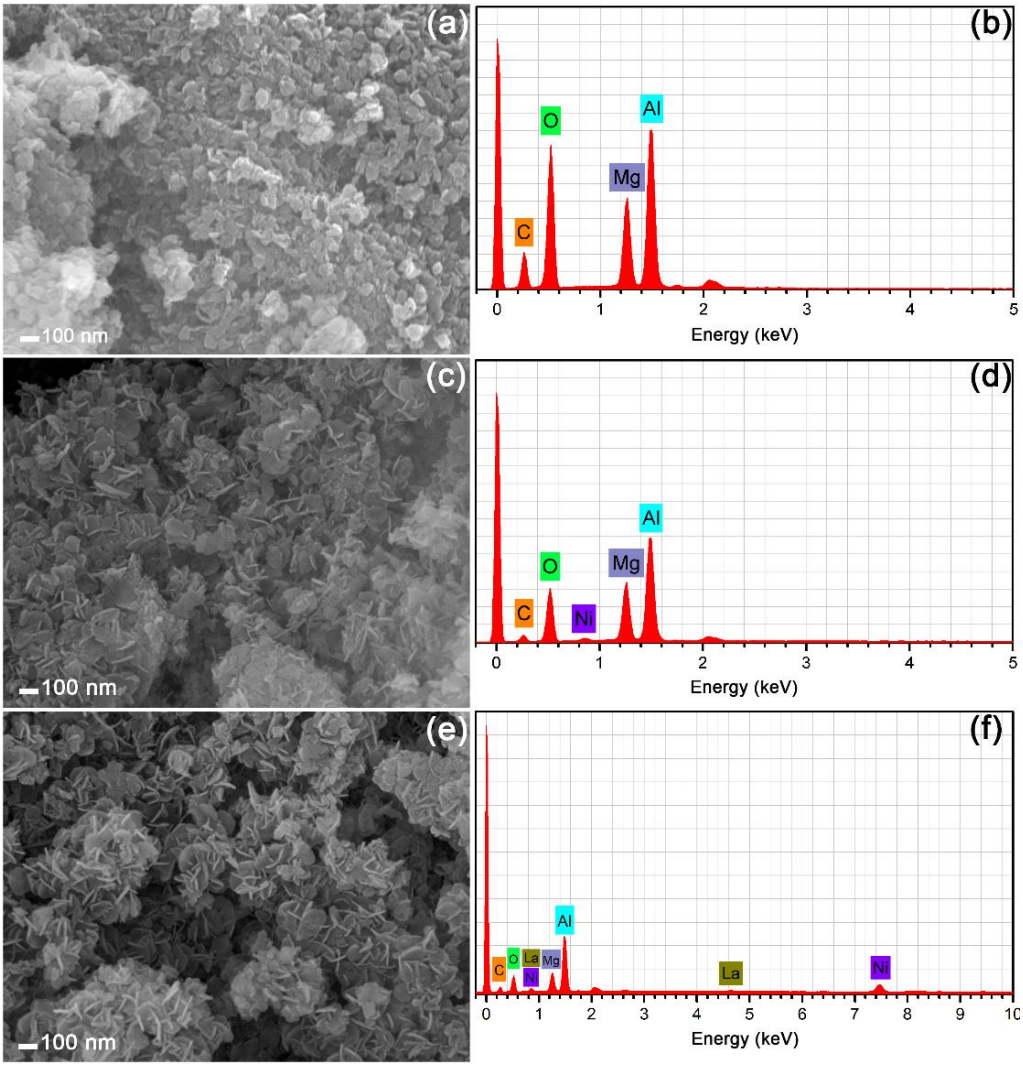

Fig. 3. FESEM-EDX images of (a) AMS-5, (b) AMS-5 EDX, (c) Ni/AMS-5, (d) Ni/AMS-5 EDX, (e) Ni-10La/AMS-5, and (f) Ni-10La/AMS-5 EDX

Brunauer–Emmett–Taylor (BET) analysis

The BET surface area, total pore volume, and average pore diameter of the supports and catalysts are summarized in Table 4. Compared with the AMS-5 support, the BET surface area of the Ni/AMS-5 catalysts decreased from 186.8 to 91.5 $m^2 \cdot g^{-1}$, which was ascribed to the fact that some of the active component Ni was loaded into the pore of the support surface. After addition of La, the BET surface area of catalysts increased from 91.5 to 130.2 and 158.4 $m^2 \cdot g^{-1}$, which was consistent with FESEM analysis. The XRD analysis showed that the introduction of La reduced the crystal size of $NiAl_2O_4$, which meant that originally blocked pores were partially exposed. The BET surface area may not be the key factor influencing the catalytic activity. Moreover, the superb catalytic performance was more determined by active components (Yu *et al*. 2019). Wu *et al*. (2013) studied the catalytic pyrolysis of biomass over Ni-Ca/Zn-Al catalysts, observing that Ni-Ca-Al (1:9) catalysts with the highest BET surface area exhibited the lowest H_2 yield, which was similar with the results in Fig. 5. Moreover, the variation trends in the total pore volume was consistent with that of the BET surface area. The average pore diameter of the AMS-

5 support, Ni/AMS-5, Ni-6La/AMS-5, and Ni-10La/AMS-5 catalysts was 12.9, 13.8, 12.1, and 13.3 nm, respectively. Catalysts with high average pore diameter can promote the reactivity of catalytic pyrolysis process because its average pore size is sufficient for gases diffusing into the active sites of catalysts for secondary cracking reaction to yield syngas (Loy *et al*. 2018).

Table 4. Textural Properties of Support and Catalysts

	BET Surface Area ($m^2 \cdot g^{-1}$)	Total Pore Volume ($cm^3 \cdot g^{-1}$)	Average Pore Diameter (nm)
AMS-5	186.85	0.55	12.86
Ni/AMS-5	91.46	0.33	13.77
Ni-6La/AMS-5	158.44	0.55	12.11
Ni-10La/AMS-5	130.17	0.49	13.26

Effect of Modified Ni/Al_2O_3 Catalysts in Pyrolysis of RS

Effect of modified supports in pyrolysis of RS

The dependence of different modified supports on the gas concentration is presented in Fig. 4, while the reaction temperature, holding time, and Ni loading was fixed at 700 °C, 20 min, and 10 wt%, respectively. As a comparison, the situation of non-catalytic pyrolysis and addition of the Ni/Al_2O_3 catalysts was also evaluated under the same reaction conditions. The syngas concentration for RS pyrolysis after addition of catalysts was always higher than RS pyrolysis alone at the same reaction conditions. The syngas concentration was increased from the smallest of 31.5 vol% (RS) to the highest of 69.2 vol% (Ni/AMS-5) when the catalysts were used. Previous literature has reported that metallic nickel can promote the tar cracking by dissociating C–O and subsequently rupturing C–H and C═C bonds, thus contributing to the syngas component (*i.e.*, H_2 and CO) formation (Matas Güell *et al*. 2011). Meanwhile, the catalysts facilitated tar dry reforming reaction (R6) towards the positive direction, which made more tar decompose into H_2 and CO. Figure 4 shows that the lower CH_4 concentration usually was associated with the higher H_2 and CO concentration, especially after using the Ni/Al_2O_3, Ni/AMS-4, and Ni/AMS-5 catalysts. This phenomenon was ascribed to these catalysts and was excellent in activating methane steam reforming (R7 and R8) and decomposition (R9). Similar results have been reached by Loy *et al.* (2018), who reported that the highest H_2 concentration associated with the lowest CH_4 concentration was obtained after introducing nickel into the pyrolysis of rice husk. Furthermore, compared with the Ni/Al_2O_3 catalysts, the Ni/AMS-5 catalysts increased syngas concentration by 14.9 vol% including 9.8 vol% H_2 and 5.1 vol% CO. These findings indicated that the Ni/AMS-5 catalysts exhibited a better catalytic activity than the Ni/Al_2O_3 catalysts in the syngas production. From Fig. 4, it can be obtained that H_2 and CO concentrations were increased from 25.6 vol% and 18.9 vol% to 40.8 vol% and 28.4 vol%, respectively, when the ratio of Al_2O_3, MgO, and SC was decreased from 5:1:1 (Ni/AMS-1) to 1:1:1 (Ni/AMS-5). In addition, the CH_4 and CO_2 concentration declined slightly with the increment of MgO and SC relative content. These results revealed that a suitable ratio of Al_2O_3, MgO, and SC could enhance CH_4 reforming reaction (R7, R8, and R10) towards the positive direction.

Tar dry reforming reaction:

$$C_nH_m + nCO_2 \rightarrow 2nCO + m/2H_2 \quad \text{(R6)}$$

CH_4 steam reforming reaction: $CH_4 + H_2O \rightarrow CO + 3H_2$ (R7)

$CH_4 + 2H_2O \rightarrow CO_2 + 4H_2$ (R8)

CH_4 decomposition: $CH_4 \rightarrow C + 2H_2$ (R9)

CH_4 dry reforming reaction: $CO_2 + CH_4 \rightarrow 2CO + 2H_2$ (R10)

Water gas shift reaction (WGS): $CO + H_2O \rightarrow H_2 + CO_2$ (R11)

The higher heating values (HHV) and lower heating values (LHV) of the gas products were calculated according to Eqs. 1 and 2 (Shahbaz *et al*. 2017). As shown in Table 5, the HHV of the gas products ranged from 9.51 to 10.57 MJ/m^3 after the addition of modified catalysts. Bridgwater (1996) reported that the average HHV of non-catalytic pyrolysis of biomass was 4 to 7 MJ/m^3. This meant that all modified catalysts can enhance the pyrolysis of RS to produce more energy. In addition, both HHV and LHV of the gas products reached maximum value when the Ni/AMS-5 catalysts were used. Consequently, compared to other catalysts, the Ni/AMS-5 catalysts were more effective for clean energy production. In contrast, the Ni/Al_2O_3 catalysts exhibited the worst activity in producing high quality fuel gas. This can be ascribed to the lower CH_4 and CO concentration after using the Ni/Al_2O_3 catalysts.

It has been revealed that in chemical manufacturing industries, such as Fischer-Tropsch synthesis, petrochemical manufacture, and bio-oil production, the H_2/CO molar ratio of syngas should be in the range of 1 to 3 (Lu and Lee 2007). From Table 5, the H_2/CO molar ratio increased from the lowest value (0.79) of non-catalytic pyrolysis to the highest value (1.43) of catalytic pyrolysis by the Ni/AMS-5 catalysts. The data indicates that the Ni/AMS-5 catalysts performed well in improving the quality of syngas similarly and were more preferable for chemical manufacturing.

$$LHV = (25.7\ H_2 + 30\ CO + 85.4\ CH_4) \times 0.0042 \quad (1)$$

$$HHV = (30.52\ H_2 + 30.18\ CO + 95\ CH_4) \times 0.0042 \quad (2)$$

In Eqs. 1 and 2, the unit of LHV and HHV is MJ/m^3; H_2, CO, and CH_4 were the volume fractions (vol%) in the fuel gas.

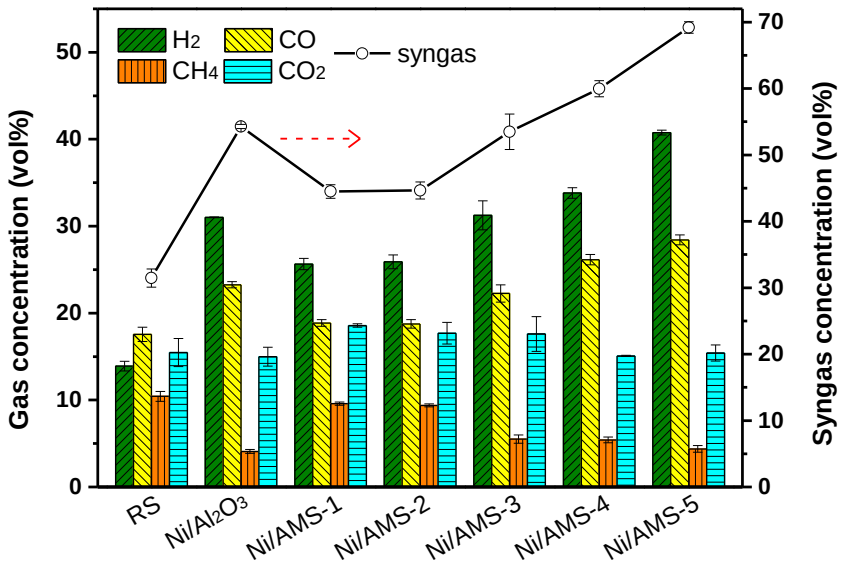

Fig. 4. Effect of support types on the concentration of H_2 (vol%) and CO (vol%)

Table 5. Gas Characteristics of RS Pyrolysis with and Without Catalysts

Catalysts	HHV (MJ/m^3)	LHV (MJ/m^3)	H_2/CO Ratio
RS	8.17	7.45	0.79
Ni/Al_2O_3	8.55	7.74	1.33
Ni/AMS-1	9.51	8.59	1.36
Ni/AMS-2	9.44	8.52	1.38
Ni/AMS-3	9.02	8.15	1.40
Ni/AMS-4	9.81	8.89	1.29
Ni/AMS-5	10.57	9.55	1.43
Ni-2La/AMS-5	11.67	10.52	1.50
Ni-4La/AMS-5	11.61	10.46	1.55
Ni-6La/AMS-5	11.63	10.48	1.54
Ni-8La/AMS-5	11.83	10.67	1.50
Ni-10La/AMS-5	12.20	11.00	1.54

Effect of doped La in pyrolysis of RS

The effect of La content on gas concentration was investigated with the Ni-xLa/AMC-5 catalysts (x = 0, 2, 4, 6, 8, and 10 wt%) at 700 °C pyrolysis temperature, 20 min holding time, and 10 wt% Ni loading. The dependence of gas concentration on La content is depicted in Fig. 5, which conveys that the syngas concentration for RS pyrolysis with the doped La catalysts was always noticeably higher than the Ni/AMC-5 catalysts at the same conditions. There was a 9.7 vol% increment of syngas concentration when the amount of added La increased from 0 to 10 wt%. In addition, while the La content was fixed at 10 wt%, the syngas concentration exhibited an optimum value of 78.9 vol% including 47.9 vol% of H_2 and 31.0 vol% of CO. As shown in Table 5, the HHV, LHV, and H_2/CO values of gas products produced from the Ni-xLa/AMS-5 catalysts were always higher than the Ni/AMS catalysts, indicating that the better quality syngas was produced. La oxycarbonate species could be formed by La reacting with CO_2 (R4) (Chen *et al*. 2019), which enhanced the consumption of CO_2 and then facilitated the WGS reaction (R11) towards the positive direction that led to the generation of more H_2. Subsequently, further reaction of $La_2O_2CO_3$ with C (R5) increased the CO concentration. Meanwhile, the partial adsorption of carbon on the surface of catalysts could be eliminated. These results indicated that the doped La performed an excellent enhancement to the activity of the Ni/AMC-5 catalysts.

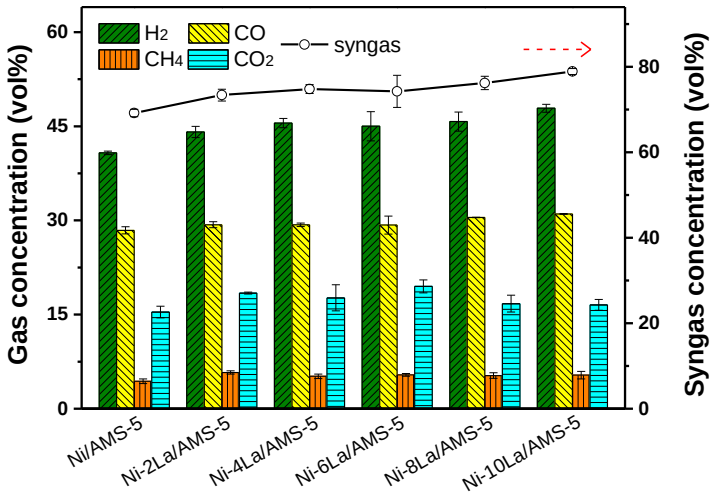

Fig. 5. Effect of La content on the concentration of H_2 (vol%) and CO (vol%)

However, there was a slow growth trend (73.3 to 78.9 vol%) of syngas concentration when the amount of added La increased from 2 to 10 wt%, which revealed that the effect of La content of Ni-xLa/AMS catalysts on syngas concentration was relatively small. The BET surface area of the Ni-xLa/AMS-5 catalysts was 156.87 (x = 2 wt%), 158.44 (x = 6 wt%), and 130.17 (x = 10 wt%), respectively. The results revealed that La had little effect on the textural properties of catalysts, leading to an apparent difference in syngas production. Thus, the Ni-10La/AMS catalysts had the best catalytic activity, but from an economical point of view, the Ni/AMS catalysts with lower amount of doped La can be selected.

Catalysts stability test

Catalysts stability is a parameter worthy of attention. As mentioned before, Ni-10La/AMS-5 catalysts exhibited the best catalytic activity. Thus, the catalytic pyrolysis experiments with Ni-10La/AMS-5 catalysts were conducted at 700 ℃ for 6 cycles (120 min) to examine the stability. Meanwhile, the Ni/Al_2O_3 catalysts were also tested as a contrast. The catalysts were not regenerated due to the limitation of laboratory conditions. Figure 6 depicts the concentration of CO and H_2 dependent on usage time of the catalysts.

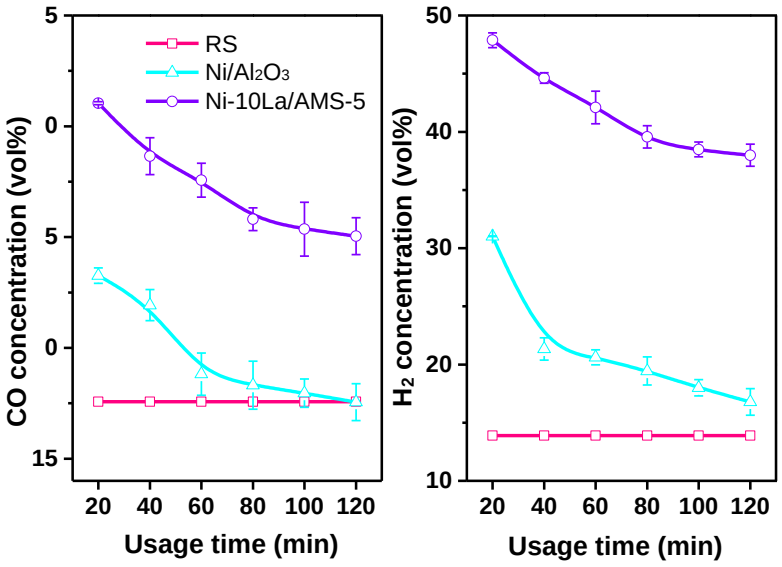

Fig. 6. Results of stability performance over the Ni/Al_2O_3 and Ni-10La/AMS-5 catalyst

It can be seen that the H_2 and CO concentration of the Ni-10La/AMS-5 catalysts were always higher than that of the Ni/Al_2O_3 catalysts during the entire process. In the first three cycles, the syngas (H_2 + CO) concentration of the Ni/Al_2O_3 and Ni-10La/AMS-5 catalysts decreased 14.8 and 9.2 vol%, respectively. The sharp drop was probably due to the adverse reaction environment. The pyrolysis furnace in this experiment was a one-stage type, and the direct contact between the catalysts and massive pyrolysis volatile gas made the catalyst easily poisoned or deactivated. In the next three cycles, the change in gas concentration was relatively small. However, after using the Ni/Al_2O_3 catalysts for 120 min, CO concentration was reduced and found to be equal to that of RS pyrolysis alone. The concentration of CO at this time using the Ni-10La/AMS-5 catalysts was even higher than that of the Ni/Al_2O_3 catalysts of the first 20 min. The H_2 concentration of the Ni/Al_2O_3 and Ni-10La/AMS-5 catalysts showed a similar trend. After the Ni-10La/AMS-5 catalysts

catalyzed for 120 min, the concentration of syngas was 63.0 vol%, which was much higher than 34.3 vol% of the Ni/Al_2O_3 catalysts. These results indicated that the Ni-10La/AMS-5 catalysts performed better in terms of stability and activity than the Ni/Al_2O_3 catalysts.

CONCLUSIONS

1. The catalytic performance of the Ni/AMS-5 and Ni-10La/AMS catalysts prepared in this experiment was better than that of the Ni/Al_2O_3 catalyst. The Ni/AMS-5 and Ni-10La/AMS catalysts increased the syngas concentration by 14.9 vol% and 24.6 vol%, respectively.
2. The optimum performance of the Ni/AMS catalysts for the production of syngas was obtained at the ratio of 1:1:1 of Al_2O_3, MgO, and SC in the support. Compared with the ratio of 5:1:1, it increased the syngas concentration 24.7 vol%, including 15.2 vol% H_2 and 9.5 vol% CO.
3. The optimum performance of the Ni-xLa/AMS-5 catalysts for the production of syngas was obtained at x = 10 wt%. Compared with the Ni/AMS-5 catalysts, it increased the syngas concentration 9.7 vol% including 7.1 vol% H_2 and 2.6 vol% CO.
4. When the amount of added La was increased from 2 to 10 wt%, the syngas concentration increased slightly from 73.3 to 78.9 vol%. From the economic point of view, the Ni/AMS catalysts with a lower amount of doped La can be selected.
5. The Ni-10La/AMS-5 catalyst was more stable than the Ni/Al_2O_3 catalysts. After the Ni-10La/AMS-5 catalysts catalyzed for 120 min, the concentration of syngas was 63.0 vol%, which was much higher than 34.3 vol% of the Ni/Al_2O_3 catalysts.

ACKNOWLEDGMENTS

The authors are grateful for the support of the Technical Innovation Major Project of Hubei Province, Grant No. 2017ABA155, the Central Committee Guides Local Science and Technology Development Special Project of Hubei Province, Grant No. 2018ZYYD062, and the Hubei Provincial Natural Science Foundation of China, Grant No. 2018CFB280.

REFERENCES CITED

Artetxe, M., Alvarez, J., Nahil, M. A., Olazar, M., and Williams, P. T. (2017). "Steam reforming of different biomass tar model compounds over Ni/Al_2O_3 catalysts," *Energy Convers. Manage.* 136, 119-126. DOI: 10.1016/j.enconman.2016.12.092

Ashok, J., and Kawi, S. (2014). "Nickel-iron alloy supported over iron–alumina catalysts for steam reforming of biomass tar model compound," *ACS Catal.* 4(1), 289-301. DOI: 10.1021/cs400621p

Beneroso, D., Bermúdez, J. M., Montes-Morán, M. A., Arenillas, A., and Menéndez, J. A. (2016). "Microwave-induced cracking of pyrolytic tars coupled to microwave

pyrolysis for syngas production," *Bioresource Technol.* 218, 687-691. DOI: 10.1016/j.biortech.2016.07.019

Bo, L. L., Wang, X. C., Wang, M. G., and Zhou, L. H. (2008). "Characteristics of carbon-supported metal catalyst prepared by microwave method," *Journal of Xi'an University of Architecture & Technology* 40(4), 532-537. DOI: 10.15986/j.1006-7930.2008.04.005

Bridgwater, A. V. (1996). "Production of high grade fuels and chemicals from catalytic pyrolysis of biomass," *Catal. Today* 29(1), 285-295. DOI: 10.1016/0920-5861(95)00294-4

Charisiou, N. D., Papageridis, K. N., Siakavelas, G., Tzounis, L., Kousi, K., Baker, M. A., Hinder, S. J., Sebastian, V., Polychronopoulou, K., and Goula, M. A. (2017). "Glycerol steam reforming for hydrogen production over nickel supported on alumina, zirconia and silica catalysts," *Top. Catal.* 60(15-16), 1226-1250. DOI: 10.1007/s11244-017-0796-y

Chen, M. Q., Li, X. J., Wang, Y. S., Wang, C. S., Liang, T., Zhang, H., Yang, Z. L., Zhou, Z. S, and Wang, J. (2019). "Hydrogen generation by steam reforming of tar model compounds using lanthanum modified Ni/sepiolite catalysts," *Energy Convers. Manage.* 184, 315-326. DOI: 10.1016/j.enconman.2019.01.066

Demirbas, A. (2009). "Political, economic and environmental impacts of biofuels: A review," *Appl. Energ.* 86(Supplement 1), S108-S117. DOI: 10.1016/j.apenergy.2009.04.036

Dong, L. S., Wu, C. F., Ling, H. J., Shi, J., Williams, P. T., and Huang, J. (2016). "Development of Fe-promoted Ni-Al catalysts for hydrogen production from gasification of wood sawdust," *Energ. Fuel.* 31(3), 2118-2127. DOI: 10.1021/acs.energyfuels.6b02050

Dong, Q., Zhang, S. P., Li, H. J., Li, X. Q., and Wang, Z. Y. (2019). "Catalytic cracking of biomass tar together with syngas production over red brick powder-supported nickel catalysts," *Fuel Process. Technol.* 194, Article ID 106123. DOI: 10.1016/j.fuproc.2019.106123

Fagbemi, L., Khezami, L., and Capart, R. (2001). "Pyrolysis products from different biomasses: Application to the thermal cracking of tar," *Appl. Energ.* 69(4), 293-306. DOI: 10.1016/S0306-2619(01)00013-7

Furusawa, T., and Tsutsumi, A. (2005). "Comparison of Co/MgO and Ni/MgO catalysts for the steam reforming of naphthalene as a model compound of tar derived from biomass gasification," *Appl. Catal. A- Gen.* 278(2), 207-212. DOI: 10.1016/j.apcata.2004.09.035

GB/T 28731 (2012). "Proximate analysis of solid biofuels," Standardization Administration of China, Beijing, China.

Guo, F. Q., Li, X. L., Liu, Y., Peng, K. Y., Guo, C. L., and Rao, Z. H. (2018). "Catalytic cracking of biomass pyrolysis tar over char-supported catalysts," *Energy Convers. Manage.* 167, 81-90. DOI: 10.1016/j.enconman.2018.04.094

He, M. Y., Xiao, B., Hu, Z. Q., Liu, S. M., Guo, X. J., and Luo, S. Y. (2009). "Syngas production from catalytic gasification of waste polyethylene: Influence of temperature on gas yield and composition," *Int. J. Hydrogen Energ.* 34(3), 1342-1348. DOI: 10.1016/j.ijhydene.2008.12.023

Hu, S., He, L. M., Wang, Y., Su, S., Jiang, L., Chen, Q. D., Liu, Q. C., Chi, H. Y., Xiang, J., and Sun, L. S.(2016). "Effects of oxygen species from Fe addition on promoting

steam reforming of toluene over Fe-Ni/Al_2O_3 catalysts," *Int. J. Hydrogen Energ.* 41(40), 17967-17975. DOI: 10.1016/j.ijhydene.2016.07.271

Huang, Y. F., Chiueh, P. T., Kuan, W. H., and Lo, S. L. (2016). "Microwave pyrolysis of lignocellulosic biomass: Heating performance and reaction kinetics," *Energy* 100, 137-144. DOI: 10.1016/j.energy.2016.01.088

Li, C., Hirabayashi, D., and Suzuki, K. (2009). "A crucial role of $O^{2-}$and O_2^{2-} on mayenite structure for biomass tar steam reforming over Ni/$Ca_{12}Al_{14}O_{33}$," *Appl. Catal. B- Environ.* 88(3-4), 351-360. DOI: 10.1016/j.apcatb.2008.11.004

Li, D. L., Ishikawa, C., Koike, M., Wang, L., Nakagawa, Y., and Tomishige, K. (2013). "Production of renewable hydrogen by steam reforming of tar from biomass pyrolysis over supported Co catalysts," *Int. J. Hydrogen Energ.* 38(9), 3572-3581. DOI: 10.1016/j.ijhydene.2013.01.057

Li, D. L., Koike, M., Chen, J., Nakagawa, Y. S., and Tomishige, K. (2014). "Preparation of Ni-Cu/Mg/Al catalysts from hydrotalcite-like compounds for hydrogen production by steam reforming of biomass tar," *Int. J. Hydrogen Energ.* 39(21), 10959-10970. DOI: 10.1016/j.ijhydene.2014.05.062

Li, D. L., Tamura, M., Nakagawa, Y. S., and Tomishige, K. (2015). "Metal catalysts for steam reforming of tar derived from the gasification of lignocellulosic biomass," *Bioresource Technol.* 178, 53-64. DOI: 10.1016/j.biortech.2014.10.010

Li, Q. Y., Ji, S. F., Hu, J. Y., and Jiang, S. (2013). "Catalytic steam reforming of rice straw biomass to hydrogen-rich syngas over Ni-based catalysts," *Chinese J. Catal.* 34(7), 1462-1468. DOI: 10.1016/S1872-2067(12)60618-4

Loy, A. C. M., Yusup, S., Lam, M. K., Chin, B. L. F., Shahbaz, M., Yamamoto, A., and Acda, M. N. (2018). "The effect of industrial waste coal bottom ash as catalyst in catalytic pyrolysis of rice husk for syngas production," *Energ. Convers. Manage.* 165, 541-554. DOI: 10.1016/j.enconman.2018.03.063

Lu, Y. J., and Lee, T. (2007). "Influence of the feed gas composition on the Fischer-Tropsch synthesis in commercial operations," *J. Nat. Gas Chem.* 16(4), 329-341. DOI: 10.1016/S1003-9953(08)60001-8

Matas Güell, B., Babich, I. V., Lefferts, L., and Seshan, K. (2011). "Steam reforming of phenol over Ni-based catalysts-A comparative study," *Appl. Catal. B- Environ*. 106(3-4), 280-286. DOI: 10.1016/j.apcatb.2011.05.012

Melo, F., and Morlanés, N. (2005). "Naphtha steam reforming for hydrogen production," *Catal. Today* (107-108), 458-466. DOI: 10.1016/j.cattod.2005.07.028

Michel, R., Lamacz, A., Krzton, A., Djéga-Mariadassou, G., Burg, P., Courson, C., and Gruber, R. (2013). "Steam reforming of α-methylnaphthalene as a model tar compound over olivine and olivine supported nickel," *Fuel* 109, 653-660. DOI: 10.1016/j.fuel.2013.03.017

Paethanom, A., Nakahara, S., Kobayashi, M., Prawisudha, P., and Yoshikawa, K. (2012). "Performance of tar removal by absorption and adsorption for biomass gasification," *Fuel Process. Technol.* 104, 144-154. DOI: 10.1016/j.fuproc.2012.05.006

Sánchez-Sánchez, M. C., Navarro, R. M., and Fierro, J. L. G. (2007). "Ethanol steam reforming over Ni/MxOy-Al_2O_3 (M=Ce, La, Zr and Mg) catalysts: Influence of support on the hydrogen production," *Int. J. Hydrogen Energ.* 32(10-11), 1462-1471. DOI: 10.1016/j.ijhydene.2006.10.025

Sehested, J. (2006). "Four challenges for nickel steam-reforming catalysts," *Catal. Today* 111(1-2), 103-110. DOI: 10.1016/j.cattod.2005.10.002

Shahbaz, M., Yusup, S., Inayat, A., Ammar, M., Patrick, D. O., Pratama, A., and Naqvi, S. R. (2017). "Syngas production from steam gasification of palm kernel shell with subsequent CO_2 capture using CaO sorbent: An aspen plus modeling," *Energ. Fuel.* 31(11), 12350-12357. DOI: 10.1021/acs.energyfuels.7b02670

Shao, S., Zhang, H., Xiao, R., Li, X., and Cai, Y. (2018). "Controlled regeneration of ZSM-5 catalysts in the combined oxygen and steam atmosphere used for catalytic pyrolysis of biomass-derivates," *Energy Convers. Manage.* 155, 175-181. DOI: 10.1016/j.enconman.2017.10.062

Sharma, Y. C., Kumar, A., Prasad, R., and Upadhyay, S. N. (2017). "Ethanol steam reforming for hydrogen production: Latest and effective catalyst modification strategies to minimize carbonaceous deactivation," *Renew. Sust. Energ. Rev.* 74, 89-103. DOI: 10.1016/j.rser.2017.02.049

Shen, Y., Liu, Y., and Yu, H. (2018). "Enhancement of the quality of syngas from catalytic steam gasification of biomass by the addition of methane/model biogas," *Int. J. Hydrogen Energ.* 43(45), 20428-20437. DOI: 10.1016/j.ijhydene.2018.09.068

Shen, Y., and Yoshikawa, K. (2013). "Recent progresses in catalytic tar elimination during biomass gasification or pyrolysis—A review," *Renew. Sust. Energ. Rev.* 21, 371-392. DOI: 10.1016/j.rser.2012.12.062

Shi, X. W., Zhang, K. D., Cheng, Q. P., Song, G. S., Fan, G. Z., and Li, J. F. (2019). "Promoting hydrogen-rich syngas production through catalytic cracking of rape straw using Ni-Fe/PAC-γAl_2O_3 catalyst," *Renew. Energ.* 140, 32-38. DOI: 10.1016/j.renene.2019.03.060

Surendar, M., Padmakar, D., Lingaiah, N., Rao, K. S. R., and Prasad, P. S. S. (2017). "Influence of La_2O_3 composition in MgO-La_2O_3 mixed oxide-supported Co catalysts on the hydrogen yield in glycerol steam reforming," *Sustain. Energ. Fuels* 1(2), 354-361. DOI: 10.1039/C6SE00023A

Świerczyński, D., Libs, S., Courson, C., and Kiennemann, A. (2007). "Steam reforming of tar from a biomass gasification process over Ni/olivine catalyst using toluene as a model compound," *Appl. Catal. B- Environ.* 74(3-4), 211-222. DOI: 10.1016/j.apcatb.2007.01.017

Tichit, D., Medina, F., Coq, B., and Dutartre, R. (1997). "Activation under oxidizing and reducing atmospheres of Ni-containing layered double hydroxides," *Appl. Catal. A-Gen.* 159(1-2), 241-258. DOI: 10.1016/S0926-860X(97)00085-9

Wang, G. Y., Xu, S. P., Wang, C., Zhang, J. J., and Fang, Z. J. (2017). "Desulfurization and tar reforming of biogenous syngas over Ni/olivine in a decoupled dual loop gasifier," *Int. J. Hydrogen Energ.* 42(23), 15471-15478. DOI: 10.1016/j.ijhydene.2017.05.041

Wang, K. Q., Dou, B. L., Jiang, B., Zhang, Q., Li, M., Chen, H. S., and Xu, Y. J. (2016). "Effect of support on hydrogen production from chemical looping steam reforming of ethanol over Ni-based oxygen carriers," *Int. J. Hydrogen Energ.* 41(39), 17334-17347. DOI: 10.1016/j.ijhydene.2016.07.261

Wang, L., Li, D. L., Koike, M., Watanabe, H., Xu, Y., Nakagawa, Y. S., and Tomishige, K. (2013). "Catalytic performance and characterization of Ni-Co catalysts for the steam reforming of biomass tar to synthesis gas," *Fuel* 112, 654-61. DOI: 10.1016/j.fuel.2012.01.073

Wu, C. F., Wang, Z. C., Huang, J., and Williams, P. T. (2013). "Pyrolysis/gasification of cellulose, hemicellulose and lignin for hydrogen production in the presence of various nickel-based catalysts," *Fuel* 106, 697-706. DOI: 10.1016/j.fuel.2012.10.064

Yang, S. X., Zhang, X. D., Chen, L., Sun, L. Z., Xie, X. P., and Zhao, B. F. (2017). "Production of syngas from pyrolysis of biomass using Fe/CaO catalysts: Effect of operating conditions on the process," *J. Anal. Appl. Pyrol.* 125, 1-8. DOI: 10.1016/j.jaap.2017.05.007

Yu, H. M., Liu, Y., Liu, J. C., and Chen, D. Z. (2019). "High catalytic performance of an innovative Ni/magnesium slag catalyst for the syngas production and tar removal from biomass pyrolysis," *Fuel* 254, Article ID 115622. DOI: 10.1016/j.fuel.2019.115622

Yu, Q.-Z., Brage, C., Nordgreen, T., and Sjöström, K. (2009). "Effects of Chinese dolomites on tar cracking in gasification of birch," *Fuel* 88(10), 1922-1926. DOI: 10.1016/j.fuel.2009.04.020

Zhang, F., Wang, M. J., Zhu, L. J., Wang, S. R., Zhou, J. S., and Luo, Z. Y. (2017). "A comparative research on the catalytic activity of La_2O_3 and γ-Al_2O_3 supported catalysts for acetic acid steam reforming," *Int. J. Hydrogen Energ.* 42(6), 3667-3675. DOI: 10.1016/j.ijhydene.2016.06.264

Zhang, R., Brown, R. C., Suby, A., and Cummer, K. (2004). "Catalytic destruction of tar in biomass derived producer gas," *Energy Convers. Manage.* 45(7-8), 995-1104. DOI: 10.1016/j.enconman.2003.08.016

Zhang, Z. K., Liu, L., Shen, B. X., and Wu, C. F. (2018). "Preparation, modification and development of Ni-based catalysts for catalytic reforming of tar produced from biomass gasification," *Renew. Sust. Energ. Rev.* 94, 1086-1109. DOI: 10.1016/j.rser.2018.07.010

Zhu, F. S., Li, X. D., Zhang, H., Wu, A. J., Yan, J. H., Ni, M. J., Zhang, H. W., and Buekens, A. (2016). "Destruction of toluene by rotating gliding arc discharge," *Fuel* 176, 78-85. DOI: 10.1016/j.fuel.2016.02.065

Article submitted: October 29, 2019; Peer review completed: January 15, 2020; Revised version received: January 29, 2020; Accepted: January 31, 2020; Published: February 10, 2020.
DOI: 10.15376/biores.15.2.2293-2309